A depth-dependent X-ray study of a $KMnF_3$ (001) surface: the order parameter at the 186 K phase transition

1994 J. Phys.: Condens. Matter 6 7189

(http://iopscience.iop.org/0953-8984/6/36/003)

J. Phys.: Condens. Matter 6 (1994) 7189–7198. Printed in the UK

A depth-dependent x-ray study of a $KMnF_3$ (001) surface: the order parameter at the 186 K phase transition

B Burandt, S Rothaug and W Press
Institut für Experimentalphysik, Universität Kiel, Olshausenstrasse 40–60, 24098 Kiel, Germany

Received 30 March 1994, in final form 1 June 1994

Abstract. In this paper we report grazing-incidence x-ray-diffraction experiments on a $KMnF_3$ (001) surface near the cubic-to-tetragonal phase transition at $T_c \simeq 186$ K. We have determined the temperature dependence of the order parameter by investigating the tetragonal strain as well as the intensity of the $\frac{7}{2}\frac{1}{2}\frac{1}{2}$ superlattice reflection. The scattering depth was controlled by the angle of incidence and varied from about 50 Å to 2500 Å. The observed strain and superlattice intensities all lie within the range of previously reported bulk values: there is no evidence for a different critical behaviour in near-surface regions as predicted by theory.

1. Introduction

Like other materials with a perovskite structure, $KMnF_3$ undergoes several structural phase transitions related to the rotation of the MnF_6 octahedra [1]. At room temperature $KMnF_3$ has the undistorted cubic perovskite structure with space group $Pm3m$. At $T_c \simeq 186$ K the softening of a Γ_{25} zone-boundary phonon leads to a structural phase transition [2]. It is characterized by a three-component order parameter with wave vector $q = (2\pi/a)(\frac{1}{2}\frac{1}{2}\frac{1}{2})$ and belongs to the $n = 3$ (Heisenberg) universality class. In this tetragonal low-temperature phase (space group $I4/mcm$) the MnF_6 octahedra are slightly antiferro-rotated around the c-axis. This rotation angle is proportional to the order parameter and increases with decreasing temperature. Within the a, b-plane as well as along the c-axis neighbouring MnF_6 octahedra are rotated alternately. This leads to a doubling of the unit cell along all lattice axes and a volume $2a_p \times 2a_p \times 2c_p$ (a_p and c_p denote the (pseudo-) cubic lattice parameters). Additionally, there is a slight tetragonal distortion ($c/a > 1$) which also increases with decreasing temperature and can be regarded as a (secondary) order parameter of the system. Although this transition should be continuous within Landau theory, it shows a slight discontinuity at a temperature T_0. T_0 is about 1 K above the critical temperature T_c obtained by extrapolation of the inverse susceptibility or similarly below T_c by extrapolation of the order parameter [3]. More precise results from renormalization-group theory predict a first-order transition [4]. The character of this transition can be changed to second order by symmetry-breaking effects, e.g. applying uniaxial stress: so there should be a tricritical point (TCP) of the Lifshitz type [5]. Indeed, experimental studies have found a TCP by applying uniaxial pressure along [110] at $p = 0.45$ kbar and two consecutive TCPs with pressure along [100] at about $p = 0.25$ kbar [6].

While there have been many experimental investigations of the bulk properties of $KMnF_3$, only few surface-sensitive studies so far have been carried out. Toennies and Vollmer [7] were the first to observe critical behaviour in near-surface regions on a cleaved

0953-8984/94/367189+10$19.50

$KMnF_3$ surface by helium-atom scattering. In particular, they found a transition temperature slightly above (varying from sample to sample) the highest reported bulk value indicating the possibility of a surface transition. From the intensity of a superlattice reflection they also observed a critical exponent much larger than in the bulk for the topmost surface layer.

In this paper we present a detailed grazing-incidence x-ray study of the depth dependence of the order parameter of a $KMnF_3$ (001) surface. By varying the angle of incidence we have determined the critical exponents for different scattering depths. First, we have investigated the tetragonal distortion. Second, the intensity of a superlattice reflection using an asymmetric grazing-incidence geometry has been determined.

2. Theoretical background

The change of the critical behaviour in near-surface regions is due to the broken translational symmetry at the surface. The missing neighbours at the surface lead to a different effective coupling constant J_1 between the surface atoms compared to the bulk value J. Detailed theoretical studies predict three different cases [8, 9]. (i) If the ratio $J_1/J < 1.5$ the phase transition in near-surface regions is driven by the bulk transition and occurs at the same critical temperature ('ordinary transition'). (ii) For $J_1/J > 1.5$ the effective coupling at the surface is so large that the surface will order at a temperature higher than the bulk value ('surface transition'). The ordering of the bulk will occur in the presence of an already ordered surface layer ('extraordinary transition'). (iii) The case of $J_1/J \simeq 1.5$ is called a 'special transition' and can be regarded as a multicritical point separating types (i) and (ii). For all of these new universality classes one finds a modified critical behaviour with new surface-related critical exponents, which can be dramatically different from the corresponding bulk values. However, the bulk correlation length ξ remains the length scale of the critical fluctuations (except in the case of the 'surface transition' where the two-dimensional correlations within the surface layer are of importance). In the case of the ordinary transition there is only one independent additional exponent, while the other surface exponents can be expressed as combinations of the new one and the bulk values via scaling relations. In theoretical studies many detailed predictions have been made also introducing new methods for precision determinations of critical parameters [10].

The first experiments were concentrated on magnetic systems and order–disorder transitions in alloys. Celotta *et al* [11] and Alvarado *et al* [12] were the first to observe surface critical behaviour of the order parameter in LEED experiments on the magnetization of Ni surfaces. A power law with the theoretically predicted critical exponent $\beta_1 = 0.825 \pm 0.04$ was found.

Surface x-ray-scattering investigations on the order–disorder transitions in Cu_3Au and, more closely related to second-order phase transitions, Fe_3Al were carried out by Dosch *et al* [13, 14]. Theoretical predictions were verified even better, as all surface exponents could be determined independently, thus allowing a successful test of the scaling relations [14].

Another test of the theoretical results was given by Burandt *et al* [15] who studied the cubic-to-tetragonal phase transition in the ionic molecular crystal NH_4Br by surface x-ray diffraction. This phase transition primarily concerns orientational order but has a strong displacive component and hence is quite different from the systems investigated so far. Within error the predictions for an ordinary transition could also be observed in this molecular crystal.

For the perovskite $KMnF_3$ many experimental as well as theoretical studies have been done concerning the structural phase transitions and the corresponding critical behaviour in

the bulk [16, 17, 18, 19]. Some of the experimental results for the structural (distortive) phase transition at 186 K are summarized in table 1. In particular, all critical exponents are found to be too small compared to the theoretical value of the $n = 3$ universality class. Furthermore, Toennies and Vollmer [7] performed a helium-atom-scattering study on a $KMnF_3$ surface. This investigation yielded an exponent $\beta_1 = 0.63 \pm 0.03$. This exponent is also too small for an ordinary transition in the Heisenberg model but in reasonable agreement with the experimental bulk values.

Table 1. Critical exponents and critical temperatures from previous reports, concerning investigations of the lattice axis $a(T)$, the tetragonal strain and the intensities of superlattice reflections. T_0 denotes the discontinuity and T_c the extrapolated critical temperature from the fits according to a continuous transition.

Reference		T_0 (K)	T_c (K)	β
Bulk				
[16]	$(c/a-1)$	187.5 ± 0.08	188.6 ± 0.07	0.260 ± 0.020
	$I(\frac{1}{2}\frac{1}{2}\frac{7}{2})$		188.0 ± 0.10	0.178 ± 0.004
	$I(\frac{1}{2}\frac{1}{2}\frac{7}{2})$		187.7 ± 0.07	0.135 ± 0.008
	$I(\frac{1}{2}\frac{1}{2}\frac{7}{2})$		187.9 ± 0.10	0.205 ± 0.005
[17]	$a(T)$	186.65	187.965 ± 0.005	0.2857 ± 0.0006
[18]	$(c/a-1)$	186.7	189.6 ± 0.30	0.316 ± 0.005
[19]	$(c/a-1)$			0.310 ± 0.005
Surface				
[7]	$I(\frac{1}{2}\frac{1}{2}0)$	191	192.8 ± 0.3	0.63 ± 0.03

3. Experimental details

In this study we have used the surface-sensitive x-ray diffraction at glancing angles. This is an excellent tool for experimental investigations of critical phenomena in near-surface regions as proposed by Dietrich and Wagner [20]. A detailed review of both theoretical and experimental aspects concerning the surface scattering is given by Dosch [21].

For x-rays the index of refraction is slightly less than unity and so the phenomenon of total external reflection occurs. Below the critical angle α_c the electromagnetic wave is exponentially damped in the z-direction and propagates along the surface. The critical angle α_c depends on the electron density of the material and the wavelength selected and lies in the range of several mrad. For a larger angle of incidence α_i the x-rays penetrate deeper into the crystal. The scattering depth Λ is given by

$$\Lambda = |\mathrm{Im}(Q_z)|^{-1}. \tag{1}$$

Here Q_z denotes the momentum transfer parallel to the surface normal inside the crystal. Within the distorted wave Born approximation (DWBA) [21], the scattering law $S(Q_z, Q_\parallel)$ is modified by the Fresnel transmission functions T_i and T_f of the incident and outgoing fields, respectively, and therefore the scattered intensity is given by

$$I = |T_i|^2 S(Q_z, Q_\parallel)|T_f|^2. \tag{2}$$

For real surfaces with perturbations of a perfectly smooth state, e.g. by surface roughness, miscut, non-crystalline surface layers etc, the structure factor has to be modified (see for example [21]). In figure 1 the scattering depth Λ is displayed as a function of the incident angle α_i and exit angle α_f. The inset shows the scattering geometry of a grazing-incidence experiment. As can be seen in figure 1, the scattering depth can also be limited for large exit angles α_f just by selecting a glancing incidence, as long as α_i lies in the range of the critical angle or below. The latter geometry is used in the asymmetric case of the grazing-incidence diffraction to study reflections with a large momentum transfer Q_z perpendicular to the surface.

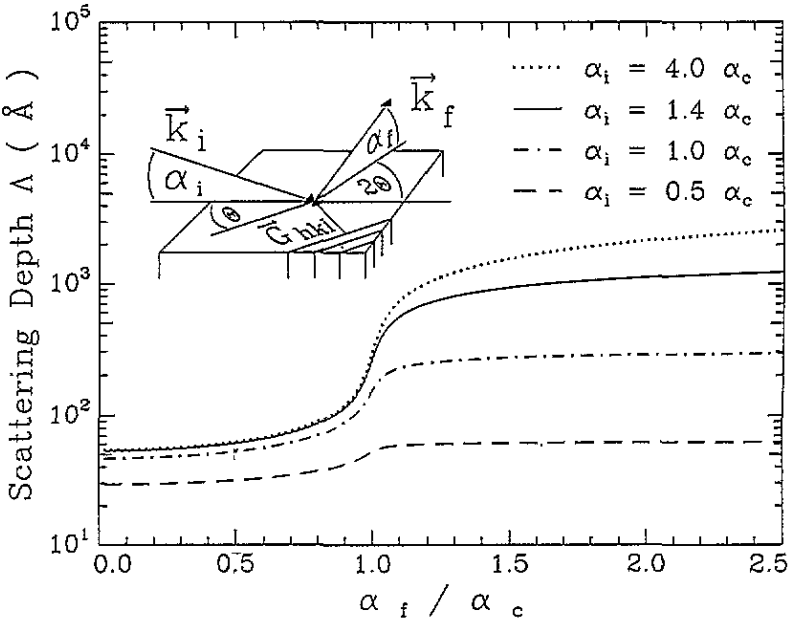

Figure 1. Scattering depth Λ for $KMnF_3$ ($\lambda = 1.54$ Å). The inset shows the grazing-incidence scattering geometry. In the asymmetric case there is a non-negligible component of the reciprocal lattice vector G_{hkl} perpendicular to the surface and therefore $\alpha_f \gg \alpha_i$. The scattering depth remains limited by the glancing incidence.

The experiments were carried out using an 18 kW Siemens rotating-anode x-ray generator with a copper target and operating at 12 kW. The white beam is monochromated by a Ge (111) crystal to select the Cu $K\alpha_1$ radiation at $\lambda = 1.54056$ Å. The beam size and divergence are controlled by a system of vertical and horizontal slits. The sample is mounted horizontally on the goniometer head of a two-circle diffractometer. The glancing incidence is realized by a slight tilt of the sample surface relative to the primary beam. For alignment the specular intensity can be determined using a NaI scintillation detector. The scattered intensity in non-specular directions is measured with a linear position-sensitive detector (PSD) which gives the option of α_f-resolved intensity profiles. The horizontal divergence of the diffracted beam is limited by two slits at a distance of 500 mm between the sample and the PSD. Because of the small scattering intensities from near-surface regions one has to find a compromise between intensity and resolution. This was done by using slit sizes of 1 mm leading to a resolution of about 2×10^{-3} Å^{-1} at the 200 Bragg peak of the $KMnF_3$ sample ($Q \simeq 3$ Å^{-1}). The spread of the glancing angle of incidence was determined to

about 0.01°.

The $KMnF_3$ sample investigated was cut from a crystal grown by R C Ward, Oxford, and was kindly provided by R Vollmer, Göttingen. It had a size of about $8 \times 8 \times 3$ mm^3 and a cleaved surface with [001] orientation. The crystalline quality proved to be excellent in the bulk as well as in near-surface regions. The temperature-dependent experiments were carried out using a helium closed-cycle cryostat in a vacuum chamber with a base pressure of about 10^{-5} mbar. The temperature stability was computer controlled within ± 0.08 K. The surface quality was also checked by investigating the specular reflectivity. Since we did not have UHV conditions, the sample surface was covered with an oxide layer and perhaps also displayed some surface disorder. It is possible that this could influence the critical behaviour but no dramatic effects would be expected as long as the correlations are short ranged [22].

4. Measurements and discussion

First, we have investigated the temperature dependence of the tetragonal strain for different scattering depths. Because none of the cubic lattice axes is preferred, at the critical temperature there will be a formation of three domains with a different orientation of the new tetragonal c-axis. This leads to a splitting of a cubic Bragg reflection into two or three peaks depending on symmetry. Additionally, those domains are slightly tilted with respect to each other [23] which gives rise to another splitting of the diffraction pattern as observed by Nicholls and Cowley [16].

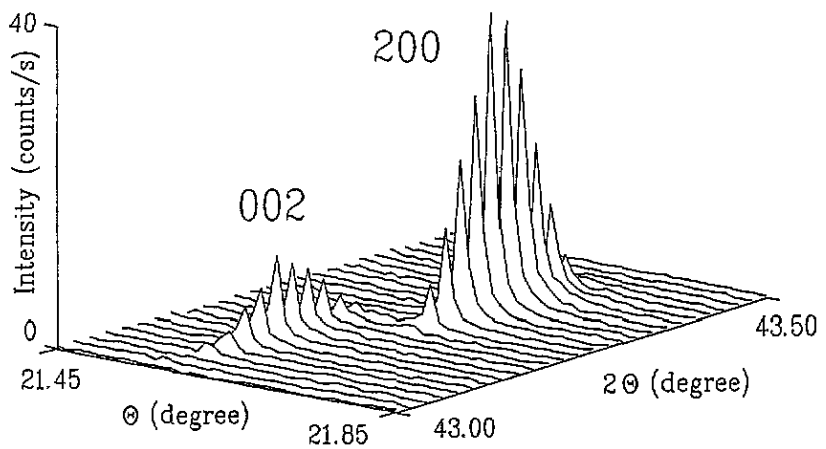

Figure 2. Diffraction plane around the 200 surface Bragg reflection (α_f integrated) in the tetragonal phase ($T = 160$ K) for a scattering depth of about 300 Å. 2Θ denotes the scattering angle, Θ the sample orientation. The different profile widths along 2Θ and Θ are caused by resolution effects.

Figure 2 shows a part of the diffraction plane around the 200 surface Bragg reflection, where 2Θ denotes the scattering angle and Θ the sample orientation. This measurement was performed well below the critical temperature for an angle of incidence of $\alpha_i \simeq 1.1\alpha_c$, i.e. a scattering depth of about 300 Å. At this surface reflection two domains are superimposed

and one finds a splitting into the 200 and 002 reflections. A further splitting due to the slight tilt of the domains as mentioned above could not be resolved. The positions of those peaks in reciprocal space also can clearly be seen in figure 3 where an α_f-integrated scan along the momentum transfer is shown. The in-plane line shapes of both reflections follow Gaussian profiles with a full width at half maximum in the range of the instrumental resolution. From the position of these peaks the size of the lattice axes and therefore the tetragonal strain can be determined directly. The exit-angle profiles of these reflections could be fitted in good agreement with the scattering law mentioned in the section above. Because of the small scattering intensities we only have considered the α_f-integrated signals in the following discussion.

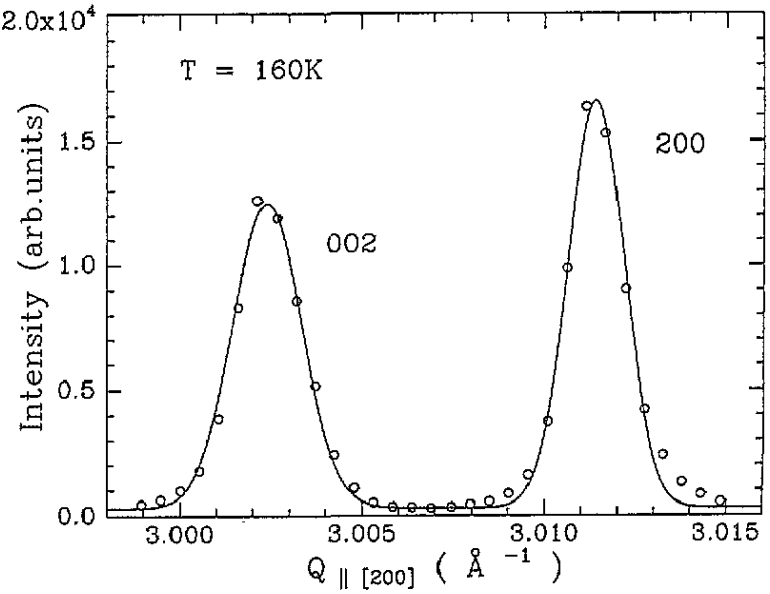

Figure 3. Splitting of the (cubic) 200 surface Bragg reflection (α_f integrated) in the tetragonal phase for a scattering depth of 300 Å. The observation of both peaks is due to the superposition of two domains. The solid line represents the fit to Gaussian line shapes.

The temperature dependence of the tetragonal distortion is shown in figure 4 for the angles of incidence of $\alpha_i \simeq 0.5\alpha_c$, $\alpha_i \simeq 0.8\alpha_c$, $\alpha_i \simeq \alpha_c$ and $\alpha_i \simeq 1.4\alpha_c$ corresponding to scattering depths of about 60 Å, 90 Å, 300 Å and 1200 Å, respectively. At a temperature $T_0 \simeq 186.5$ K a slight discontinuity can be noted limiting the further approach of T_c. This also causes an insurmountable problem in determining the exact value of T_c experimentally. When treating the transition as continuous (as has been done in many cases, e.g. [16] or other references in table 1), T_c has to be taken as a numerical parameter in the fit procedure. As can be seen in a log–log plot of the data (figure 4) we find the temperature behaviour according to a power law

$$\left(\frac{c}{a} - 1\right) \propto \left(\frac{T_c - T}{T_c}\right)^{2\beta}. \tag{3}$$

We have fitted this power law to the data in two ways: while in model 1 the critical temperature was assumed to be the same for all scattering depths, it was allowed to vary in model 2. The results of the critical temperatures and exponents β obtained are summarized

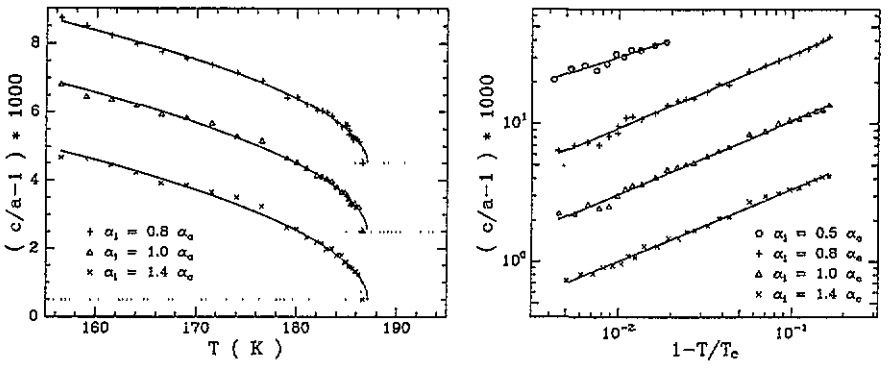

Figure 4. Temperature dependence of the tetragonal strain for different scattering depths. The solid lines are fits to a power law (model 2, see text and table 2). Left: linear scale; right: log–log plot.

in table 2. All values of the critical exponents within error agree with the bulk values reported by other authors (compare table 1). In particular, there is no hint towards a significant change with the scattering depth of either the critical exponent or the transition temperature.

Table 2. Critical exponents from the tetragonal strain for different angles of incidence α_i, i.e. different scattering depths Λ. In model 1 the transition temperature was the same for all scattering depths while in model 2 the transition temperature was fitted separately for each data set.

		Model 1		Model 2	
α_i/α_c	Λ (Å)	T_c (K)	β	T_c (K)	β
0.5	60	187.07 ± 0.08	0.214 ± 0.021	186.99 ± 0.77	0.204 ± 0.096
0.8	90		0.268 ± 0.007	187.04 ± 0.15	0.265 ± 0.011
1.1	300		0.268 ± 0.007	187.05 ± 0.14	0.266 ± 0.011
1.5	1200		0.257 ± 0.007	187.14 ± 0.14	0.262 ± 0.009

The theoretically expected values for this system according to the Heisenberg model should be $\beta = 0.365$ in the bulk and $\beta_1 = 0.85$ in near-surface regions. The reported small critical exponents may be due to the neighbourhood of a tricritical point (see section 1) with a (mean-field) bulk exponent of $\beta = 0.25$ or a Lifshitz-type TCP with an exponent β between $\frac{1}{6}$ and $\frac{1}{8}$ [5]. Another, more probable explanation is the fact that the data are related to a transition, which actually is discontinuous, but is described by a power law according to the theory of continuous phase transitions: within Landau theory this may lead to an exponent β somewhere between 0.25 and 0.125, as shown e.g. by Hüller and Press [24].

We have also studied the critical behaviour by the investigation of the intensity of a superlattice reflection. Due to the symmetry of the (001) surface no superlattice reflections are observable in this plane. Therefore an asymmetric grazing-incidence geometry ($\alpha_i < \alpha_c$, $\alpha_f \gg \alpha_c$) was chosen to analyse the $\frac{7}{2}\frac{1}{2}\frac{1}{2}$ reflection. Because of the large exit angle, the Fresnel transmissivity of the outgoing beam is $T_f = 1$ and so the α_f-profiles showed a Gaussian distribution determined by the instrumental resolution. As mentioned above, only integrated intensities are considered in the following.

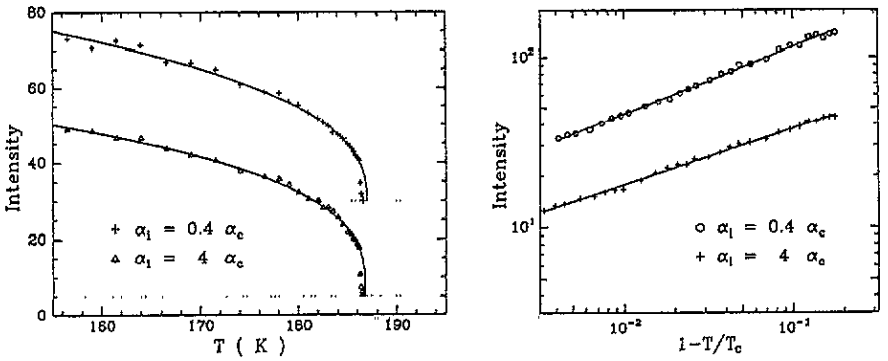

Figure 5. Temperature dependence of the integrated intensity of the $\frac{7}{2}\frac{1}{2}\frac{1}{2}$ superlattice reflection for two different scattering depths. The solid lines are fits to a power law (model 2, see table 3). Left: linear scale; right: log–log plot.

The integrated intensity of this superlattice peak is shown in figure 5 for two different angles of incidence, $\alpha_i \simeq 0.4\alpha_c$ and $\alpha_i \simeq 4\alpha_c$ .They correspond to scattering depths of about 50 Å and 2500 Å, respectively. The data can also be fitted by a power law

$$I \propto \left(\frac{T_c - T}{T_c}\right)^{2\beta} \tag{4}$$

as shown in figure 5 using the same critical-temperature- (model 1) or depth-dependent values (model 2). The results are listed in table 3. The exponents so obtained are even smaller than those determined from the tetragonal strain. Yet they also are in agreement with previous reports for the bulk (see table 1). However, there is a serious problem in determining critical exponents of $KMnF_3$ from the intensity of a superlattice peak: because the relative population of the different domains can also be a function of temperature [25], the real critical behaviour may be hidden in the experimental data as long as the scattering volume contains many domains. But the formation of differently oriented domains may also be suppressed by applying uniaxial stress for example by a special mounting of the sample.

Table 3. Critical exponents from the integrated intensity of the $\frac{7}{2}\frac{1}{2}\frac{1}{2}$ superlattice reflection for different angles of incidence α_i, i.e. different scattering depths Λ. In model 1 the transition temperature was the same for all scattering depths while in model 2 the transition temperature was fitted separately for each data set.

		Model 1		Model 2	
α_i/α_c	Λ (Å)	T_c (K)	β	T_c (K)	β
0.4	50	186.91 ± 0.05	0.195 ± 0.003	186.97 ± 0.07	0.198 ± 0.004
4	2500		0.168 ± 0.003	186.83 ± 0.07	0.164 ± 0.003

5. Conclusion

In conclusion, we have found no evidence for a depth dependence of the critical behaviour of the order parameter at the $KMnF_3$ (001) surface. Contrary to the study of Toennies and Vollmer, who observed a critical exponent $\beta \simeq 0.63$ at the topmost layer [7], our results all

lie within the range of previously reported bulk values from 0.16 to 0.27. Also we have *not* found a shift of the critical temperature towards higher values for small scattering depths as reported by these authors. These results may have been influenced by some problems: (i) the description of an actually discontinuous phase transition in terms of a continuous one, (ii) the impossibility of measuring the critical temperature, experimentally, (iii) the influence of an oxide, a non-crystalline layer or generally impurities on the surface; the latter should be negligible as long as the correlations are of short-range order and decrease proportionally to r^{-l} with $l > 1.5$ [22] and, finally, (iv) according to the discontinuity, the correlation length near T_0 remains finite and perhaps is too small compared to the scattering depth. Only if the correlation length lies in the range of the scattering depth will one find a crossover from critical bulk to surface behaviour [21]. However, according to the experimental data of Nicholls and Cowley [16] one can approximate the correlation length to about 150 Å at a temperature of 5 K below T_c. This lies well in the range of the smallest scattering depth and therefore a crossover should have been seen.

Finally, the modified critical behaviour may be restricted for an unknown reason to the uppermost surface layer. So, also in the case of the smallest scattering depth of about 50 Å the bulk signal may cover the weak surface intensity.

Acknowledgments

We would like to thank R Vollmer for providing the sample. We are also indebted to S Dietrich and F Wagner for helpful discussions. This work has been supported by the Bundesminister für Forschung und Technologie under the contract numbers 05 401 ABI 2 and 05 5F KABB.

References

[1] Cowley R A 1980 *Adv. Phys.* **29** 1
[2] Gesi K, Axe J D, Shirane G and Linz A 1972 *Phys. Rev.* B **5** 1933
[3] Bruce A D 1980 *Adv. Phys.* **29** 111
[4] Aharony A 1980 *Ferroelectrics* **24** 313
[5] Aharony A and Bruce A D 1979 *Phys. Rev. Lett.* **42** 462
[6] Stokka S, Fossheim K and Samulionis V 1981 *Phys. Rev. Lett.* **47** 1740
[7] Toennies J P and Vollmer R 1991 *Phys. Rev.* B **44** 9833
[8] Binder K 1983 *Phase Transitions and Critical Phenomena* vol 8, ed C Domb and J L Lebowitz (London: Academic)
[9] Diehl H W 1983 *Phase Transitions and Critical Phenomena* vol 10, ed C Domb and J L Lebowitz (London: Academic)
[10] Ruge C, Dunkelmann S and Wagner F 1992 *Phys. Rev. Lett.* **69** 2465
[11] Celotta R J, Pierce D T, Wang G C, Bader S C and Felcher G P 1979 *Phys. Rev. Lett.* **43** 728
[12] Alvarado S F, Campagna M and Hopster 1982 *Phys. Rev. Lett.* **48** 51
[13] Dosch H, Mailänder L, Reichert H, Peisl J and Johnson R L 1991 *Phys. Rev.* B **43** 13 172
[14] Dosch H, Mailänder L, Johnson R L and Peisl J 1992 *Surf. Sci.* **279** 367
[15] Burandt B, Press W and Haussühl S 1993 *Phys. Rev. Lett.* **71** 1188
[16] Nicholls U J and Cowley R A 1987 *J. Phys. C: Solid State Phys.* **20** 3417
[17] Sakashita H, Ohama N and Okazaki A 1981 *J. Phys. Soc. Japan* **50** 4013
[18] Gibaud A, Shapiro S M, Nouet J and You H 1991 *Phys. Rev.* B **44** 2437
[19] Ratuszna A 1993 *J. Phys.: Condens. Matter* **5** 841
[20] Dietrich S and Wagner H 1983 *Phys. Rev. Lett.* **51** 1469
[21] Dosch H 1992 *Critical Phenomena at Surfaces and Interfaces (Evanescent x-ray and Neutron Scattering) (Springer Tracts in Modern Physics 126)* (Berlin: Springer)
[22] Diehl H W and Nuesser A 1990 Z. *Phys.* B **79** 69
[23] Gibaud A, Ryan T W and Nelmes R J 1987 *J. Phys. C: Solid State Phys.* **20** 3833

[24] Hüller A and Press W 1979 *The Plastically Crystalline State* ed J N Sherwood (New York: Wiley)
[25] Tietze H, Müllner M and Jex H 1981 *Phys. Status Solidi* a **66** 239